

**NASA TECHNICAL
MEMORANDUM**



NASA TM X-892
X68 16001

NASA TM X-892

(NASA-TM-X-892) STATIC LONGITUDINAL AND
LATERAL AERODYNAMIC CHARACTERISTICS AT MACH
NUMBERS OF 1.41 AND 2.20 OF A VARIABLE
SWEEP AIRPLANE CONFIGURATION HAVING BODY
G.V. Foster (NASA) Sep. 1963 28 p

N72-73189

Unclas
CG/99 31929

**STATIC LONGITUDINAL AND LATERAL
AERODYNAMIC CHARACTERISTICS AT
MACH NUMBERS OF 1.41 AND 2.20 OF
A VARIABLE-SWEEP AIRPLANE
CONFIGURATION HAVING BODY-MOUNTED
NACELLES WITH CONICAL INLETS**

*By Gerald V. Foster;
Langley Research Center,
Langley Station, Hampton, Va.*

NATIONAL AERONAUTICS AND SPACE ADMINISTRATION • WASHINGTON, D. C. • SEPTEMBER 1963

REPRODUCED BY
NATIONAL TECHNICAL
INFORMATION SERVICE
U.S. DEPARTMENT OF COMMERCE
SPRINGFIELD, VA. 22161

TECHNICAL MEMORANDUM X-892

STATIC LONGITUDINAL AND LATERAL AERODYNAMIC
CHARACTERISTICS AT MACH NUMBERS OF 1.41 AND 2.20
OF A VARIABLE-SWEEP AIRPLANE CONFIGURATION HAVING
BODY-MOUNTED NACELLES WITH CONICAL INLETS

By Gerald V. Foster

Langley Research Center
Langley Station, Hampton, Va.

GROUP 4
Downgraded at 3 year intervals;
declassified after 12 years

NATIONAL AERONAUTICS AND SPACE ADMINISTRATION

NATIONAL AERONAUTICS AND SPACE ADMINISTRATION

TECHNICAL MEMORANDUM X-892

STATIC LONGITUDINAL AND LATERAL
AERODYNAMIC CHARACTERISTICS AT MACH NUMBERS OF 1.41
AND 2.20 OF A VARIABLE-SWEEP AIRPLANE CONFIGURATION
HAVING BODY-MOUNTED NACELLES WITH CONICAL INLETS*

By Gerald V. Foster

SUMMARY

The longitudinal and lateral aerodynamic characteristics of a variable-sweep airplane configuration have been investigated in the Langley 4- by 4-foot supersonic pressure tunnel at Mach numbers of 1.41 and 2.20. The configuration employed body-mounted nacelles with conical-spike inlets and was tested with various nacelle arrangements and with wing sweep angles of both 65° and 80° .

The results indicated reasonably linear longitudinal stability and control characteristics. The maximum untrimmed values of lift-drag ratio were relatively low for all complete configurations, being in the range from about 4.7 to 5.3. None of the nacelle arrangements investigated caused any decrease in maximum lift-drag ratio, however, and one arrangement provided a small increase in lift-drag ratio resulting from a favorable effect on drag due to lift. The complete configurations had a positive effective dihedral and a reasonably high level of directional stability that was essentially invariant with angle of attack.

INTRODUCTION

The NASA is currently conducting studies directed toward the development of multimission fighter airplanes incorporating variable-wing sweep as a means of combining efficient subsonic and supersonic flight characteristics. (See ref. 1.) The airplane is to be capable of performing a mission which entails short-field take-off and landing, a long range for subsonic ferrying or loitering, and low-altitude supersonic flight.

This paper extends the results of the general study of multimission aircraft to include a variable-sweep airplane configuration having twin external body-mounted engine nacelles with conical inlets and conventional tail surfaces. Wing sweep angles of 65° and 80° were studied in order to cover the range of interest

*Title, Unclassified.

at supersonic speeds. The investigation was made in the Langley 4- by 4-foot supersonic pressure tunnel and includes both the longitudinal and lateral stability characteristics for various configurations. Aerodynamic characteristics of this model are presented in reference 2.

SYMBOLS

Force and moment coefficients presented herein are referred to the body-axis system except for lift and drag coefficients, which are referred to the wind-axis system. The coefficients are based on the wing geometry of the respective configurations. The moment reference is located at a station corresponding to 51.6 percent and 51.0 percent of the body length for wing sweeps of 65° and 80° , respectively.

b wing span

C_D drag coefficient, $\frac{\text{Drag}}{qS}$

C_L lift coefficient, $\frac{\text{Lift}}{qS}$

C_l rolling-moment coefficient, $\frac{\text{Rolling moment}}{qSb}$

C_{l_β} effective-dihedral parameter, $\frac{\partial C_l}{\partial \beta}$

C_m pitching-moment coefficient, $\frac{\text{Pitching moment}}{qS\bar{c}}$

C_n yawing-moment coefficient, $\frac{\text{Yawing moment}}{qSb}$

C_{n_β} directional-stability parameter, $\frac{\partial C_n}{\partial \beta}$

C_Y side-force coefficient, $\frac{\text{Side force}}{qS}$

C_{Y_β} side-force parameter, $\frac{\partial C_Y}{\partial \beta}$

\bar{c} wing mean geometric chord

L/D	lift-drag ratio, $\frac{C_L}{C_D}$
$(L/D)_{\max}$	maximum lift-drag ratio
M	Mach number
q	free-stream dynamic pressure
S	wing area including intercept
α	angle of attack, deg
β	angle of sideslip, deg
δ_h	horizontal-tail deflection, deg
Λ	sweep angle of leading edge of outboard wing panel, deg

Components:

B	body
W	wing
V	vertical tail
H	horizontal tail
N	nacelle

MODEL AND APPARATUS

Details of the model are presented in figure 1 and table I. The model was provided with interchangeable wings having the outer panels swept back 65° and 80° . In addition, the tail surfaces and nacelles were designed in a manner that permitted testing various combinations of components.

TESTS, CORRECTIONS, AND ACCURACY

The test conditions were as follows:

Mach number	1.41	2.20
Reynolds number based on \bar{c} of 80° swept wing	1.51×10^6	1.13×10^6
Stagnation pressure, lb/sq ft	1,440	1,440
Stagnation temperature, $^\circ\text{F}$	110	110

The stagnation dewpoint was maintained sufficiently low (-25° or less) to prevent condensation effects in the test section. The angles of attack and side-slip were corrected for deflection of the balance and sting under load. The pressure measurements were made at the annulus of the nacelle base and within the balance chamber. The drag force was adjusted so that nacelle base pressure and balance-chamber pressure corresponded to free-stream static pressure. The nacelle exits were equipped with cylindrical plugs having a conical forebody to provide approximately choked exit conditions. These plugs were supported from the model, and hence no base drag due to the plugs was measured by the balance. The exit pressures were measured by two static-pressure tubes and twelve total-pressure tubes. The internal drag of the nacelles was then determined from the change in momentum from free-stream conditions to conditions measured at the nacelle exit. The internal-drag-coefficient corrections for the various nacelle arrangements, based on the geometry of the 65° swept wing, are as follows:

Nacelle	Internal drag coefficient at -	
	M = 1.41	M = 2.20
Small horizontal outboard	0.0022	0.0052
Small horizontal inboard	-----	.0052
Small lower outboard	-----	.0052
Large horizontal outboard	-----	.0059

Change in sweep of the outer wing panels from 65° to 80° had no effect on the internal drag of the small horizontal outboard nacelles. The nacelle exit plugs introduced an interference on the nacelles which resulted in a decrease in the drag level of the model. Estimates indicate that the drag coefficient of the 65° swept-wing configuration at $\alpha = 0^{\circ}$ and $M = 2.20$ would be as much as 0.0010 greater if these interference effects were accounted for. In order to assure a turbulent boundary layer, a $1/8$ -inch band of No. 80 carborundum grains was applied to the wing and tail surfaces at 5 percent of the local chord. Similar roughness was applied to the body, nacelles, and nacelle struts.

The estimated accuracy of the data, reduced to coefficients on the basis of the geometry of the 80° swept wing, is as follows:

	M = 1.41	M = 2.20
C_L	± 0.0046	± 0.0064
C_D	± 0.0003	± 0.0005
C_m	± 0.0010	± 0.0014
C_l	± 0.0003	± 0.0004
C_n	± 0.0009	± 0.0012
C_Y	± 0.0046	± 0.0064
α , deg	± 0.1	± 0.1
β , deg	± 0.1	± 0.1
δ_h , deg	± 0.1	± 0.1

RESULTS

The results of this investigation are presented in the following figures:

Figure

Longitudinal Characteristics:

Effects of various components; $\Lambda = 80^\circ$; $M = 1.41$	2
Effect of horizontal-tail deflection; $\Lambda = 80^\circ$; $M = 1.41$	3
Effect of horizontal-tail deflection; $\Lambda = 65^\circ$; $M = 2.20$	4
Effect of horizontal-tail deflection; $\Lambda = 80^\circ$; $M = 2.20$	5
Effect of various nacelles; $\Lambda = 65^\circ$; $M = 2.20$	6

Lateral Characteristics:

Effect of vertical tail on lateral aerodynamic characteristics of model; $\Lambda = 65^\circ$; $M = 2.20$	7
Effect of vertical and horizontal tails on lateral stability derivatives; $\Lambda = 80^\circ$; $M = 1.41$	8
Effect of vertical tail on lateral stability derivatives; $\Lambda = 65^\circ$; $M = 2.20$	9
Effect of vertical and horizontal tails on lateral stability derivatives; $\Lambda = 80^\circ$; $M = 2.20$	10

The longitudinal stability and control characteristics are reasonably linear for each configuration investigated (figs. 3 to 6). Maximum untrimmed values of L/D are relatively low for all complete configurations, being in the range from about 4.7 to 5.3. Results obtained by varying the nacelle size and position for the 65° wing configuration at $M = 2.20$ (fig. 6) indicate that each nacelle arrangement provides an increase in lift but has little effect on the longitudinal stability characteristics. It is interesting to note that none of the nacelle arrangements investigated caused any decrease in $(L/D)_{\max}$, and the small horizontal inboard nacelle provided a small increase in L/D resulting from a favorable effect on drag due to lift.

The lateral aerodynamic characteristics presented in figure 7 are typical of the linearity of all the basic sideslip data. Sideslip derivatives obtained from the basic data (figs. 8 to 10) indicate positive effective dihedral and a reasonably high level of directional stability that is essentially invariant with angle of attack. The directional characteristics apparently result from favorable effects of the nacelle installation (fig. 9). Increasing the wing sweep from 65° to 80° at $M = 2.20$ (figs. 9 and 10) resulted in an increase in directional stability and in the positive dihedral effect.

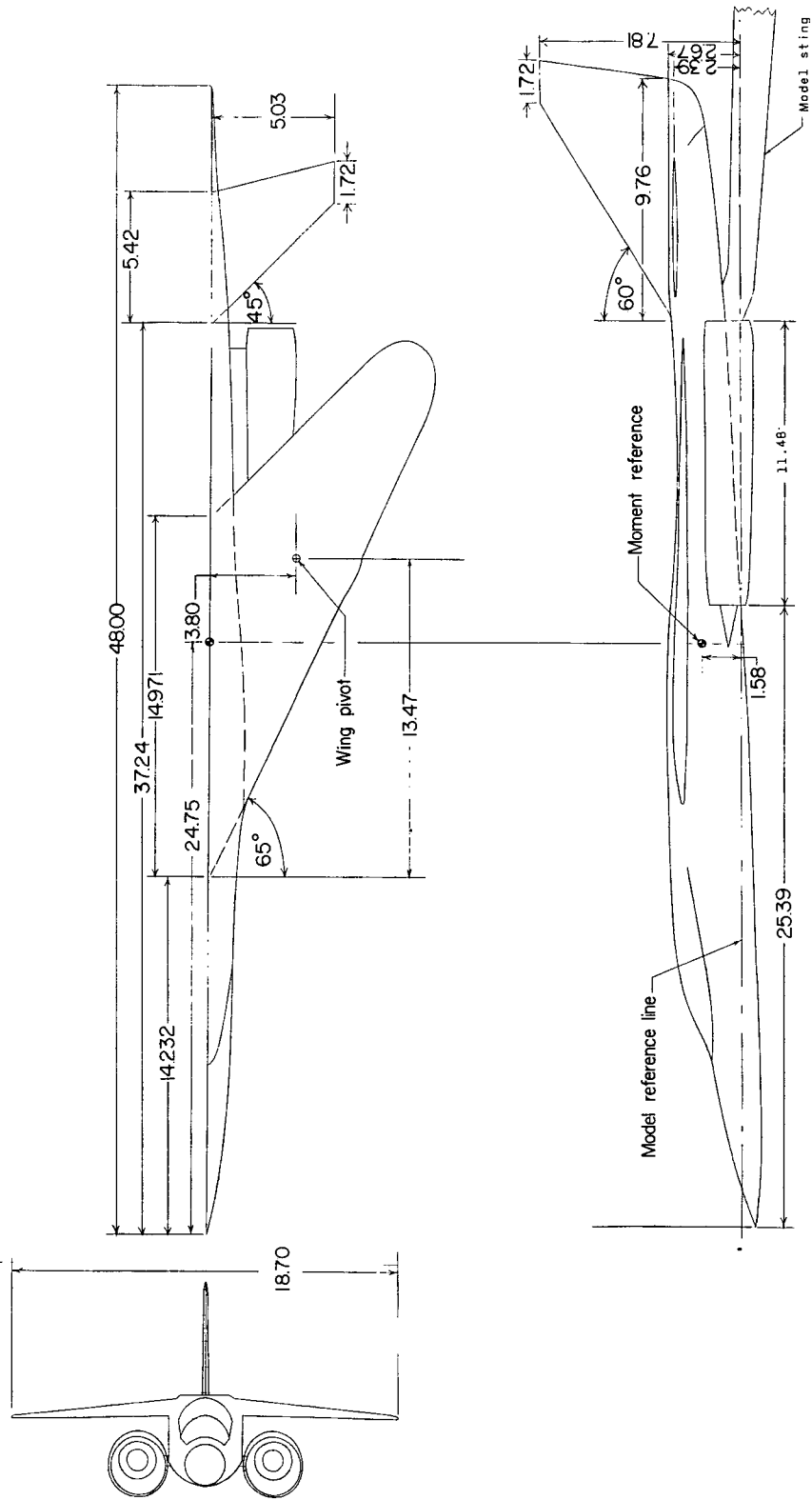
Langley Research Center,
National Aeronautics and Space Administration,
Langley Station, Hampton, Va., June 27, 1963.

REFERENCES

1. Polhamus, Edward C., and Hammond, Alexander D.: Aerodynamic Research Relative to Variable-Sweep Multimission Aircraft. Ch. II of Compilation of Papers Summarizing Some Recent NASA Research on Manned Military Aircraft. NASA TM X-420, 1960, pp. 13-38.
2. Capone, Francis J., and Lee, Edwin E., Jr.: Transonic Aerodynamic Characteristics of Three V/STOL Fighter Airplane Models With Variable-Sweep or Skewed Wings and Different Engine Installations. NASA TM X-706, 1962.

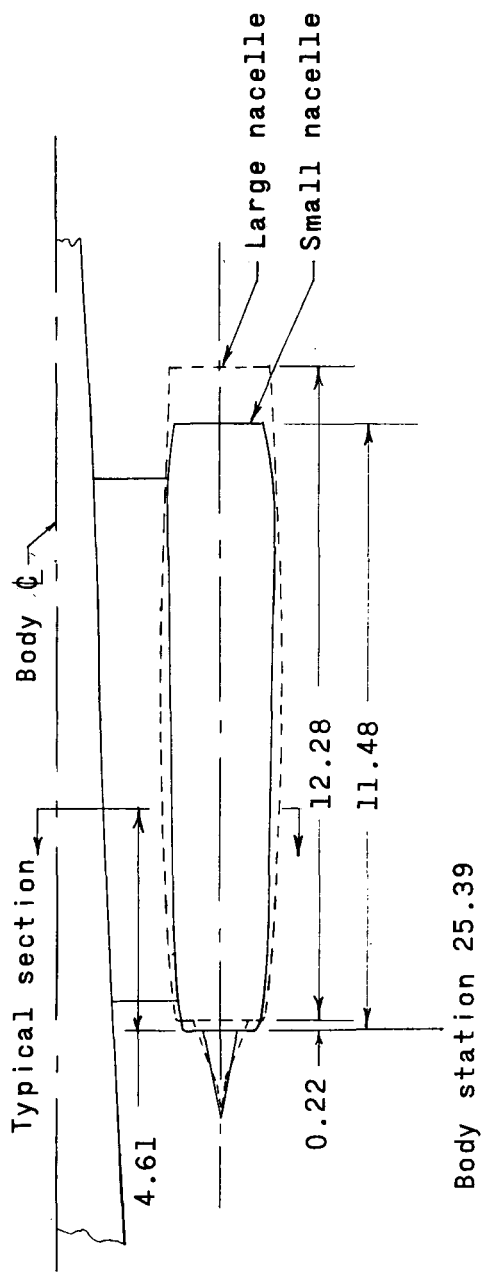
TABLE I.- GEOMETRIC CHARACTERISTICS OF MODEL

Wing:		
Leading-edge sweep, deg	65	80
Span, in.	18.70	14.73
Area, sq ft	1.230	1.208
Mean aerodynamic chord, in.	10.85	12.80
Incidence, deg	1.0	1.0
Airfoil section, normal to T.E.	64A207	64A207
Horizontal tail:		
Leading-edge sweep, deg	45	
Span, in.	10.06	
Taper ratio	0.34	
Area, sq ft	0.213	
Dihedral	0	
Airfoil section	65A003	
Vertical tail:		
Leading-edge sweep, deg	60	
Span, in.	5.14	
Taper ratio	0.177	
Area, sq ft	0.205	
Nacelles:		
Small		
Inlet capture area, sq ft	0.0123	
Duct exit area (no choke), sq ft	0.0123	
Duct exit area (with choke), sq ft	0.0107	
Large		
Inlet capture area, sq ft	0.0154	
Duct exit area (no choke), sq ft	0.0154	
Duct exit area (with choke), sq ft	0.0118	

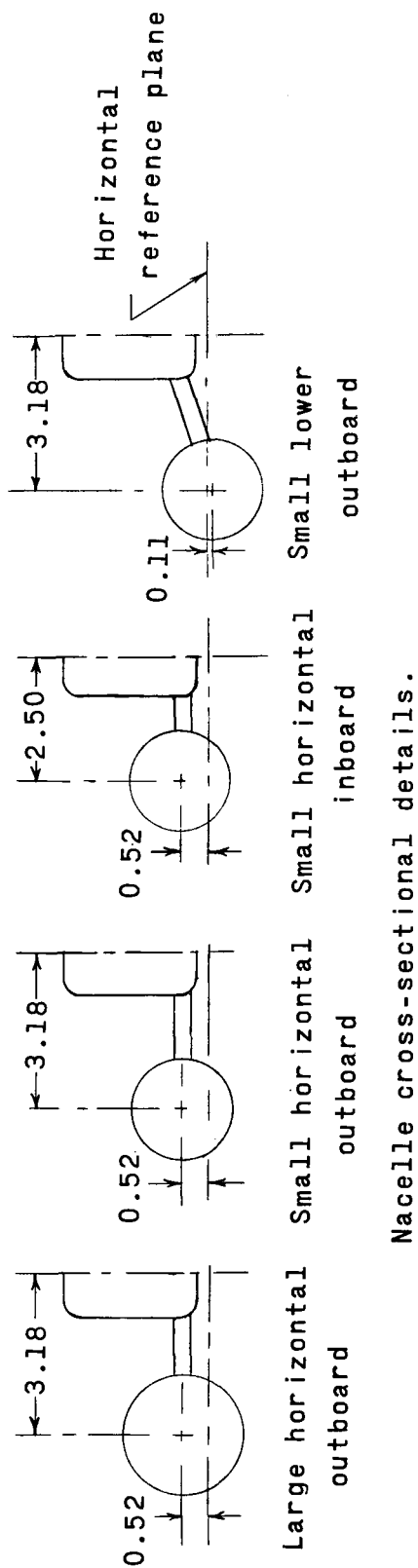


(a) Complete configuration.

Figure 1.- Details of model. All dimensions are in inches unless otherwise noted.



Plan view of nacelles



(b) Nacelles.

Figure 1.- Concluded.

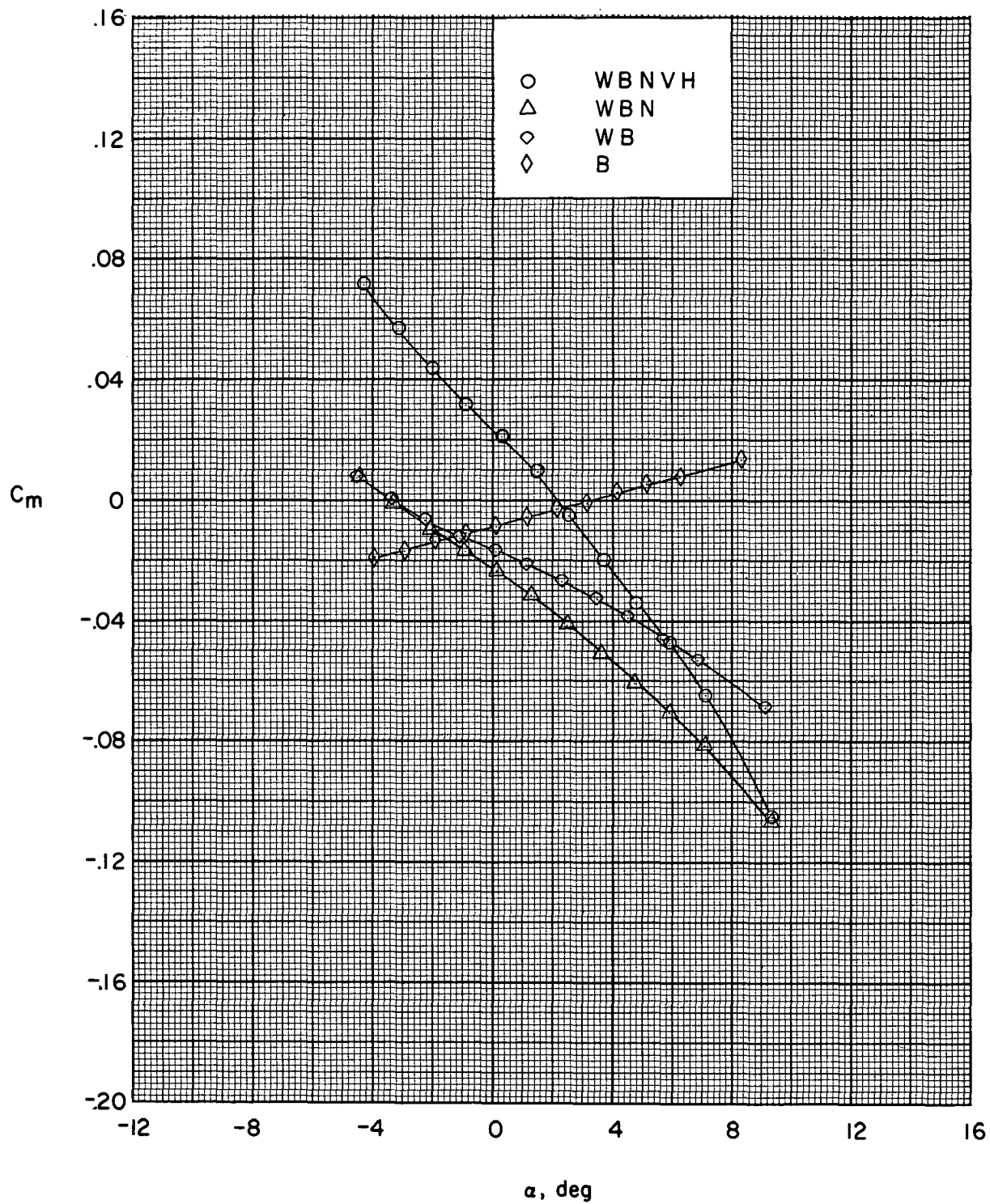


Figure 2.- Longitudinal aerodynamic characteristics for various combinations of model components.
 $\Lambda = 80^\circ$; small horizontal outboard nacelle. $M = 1.41$.

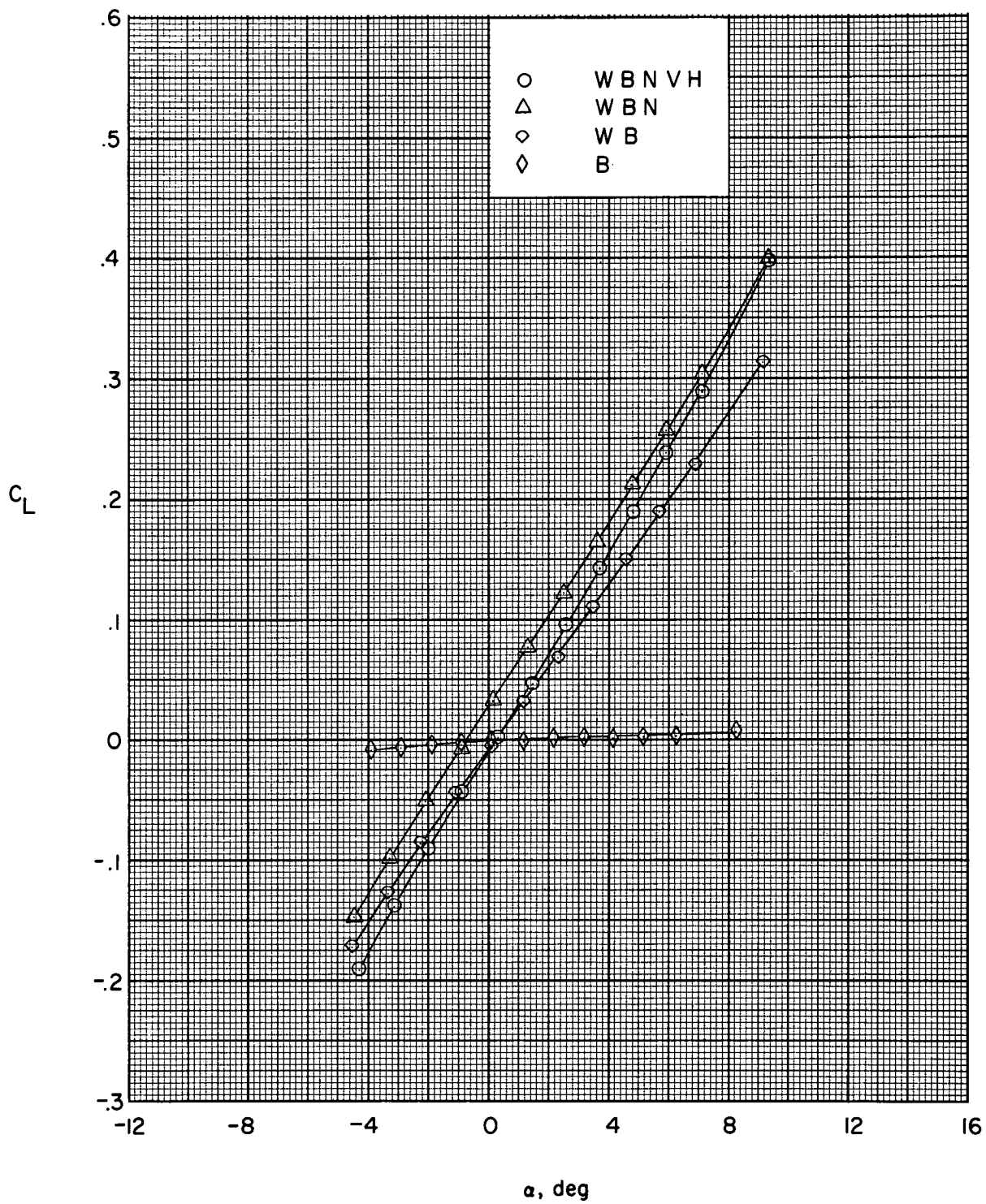


Figure 2.- Continued.

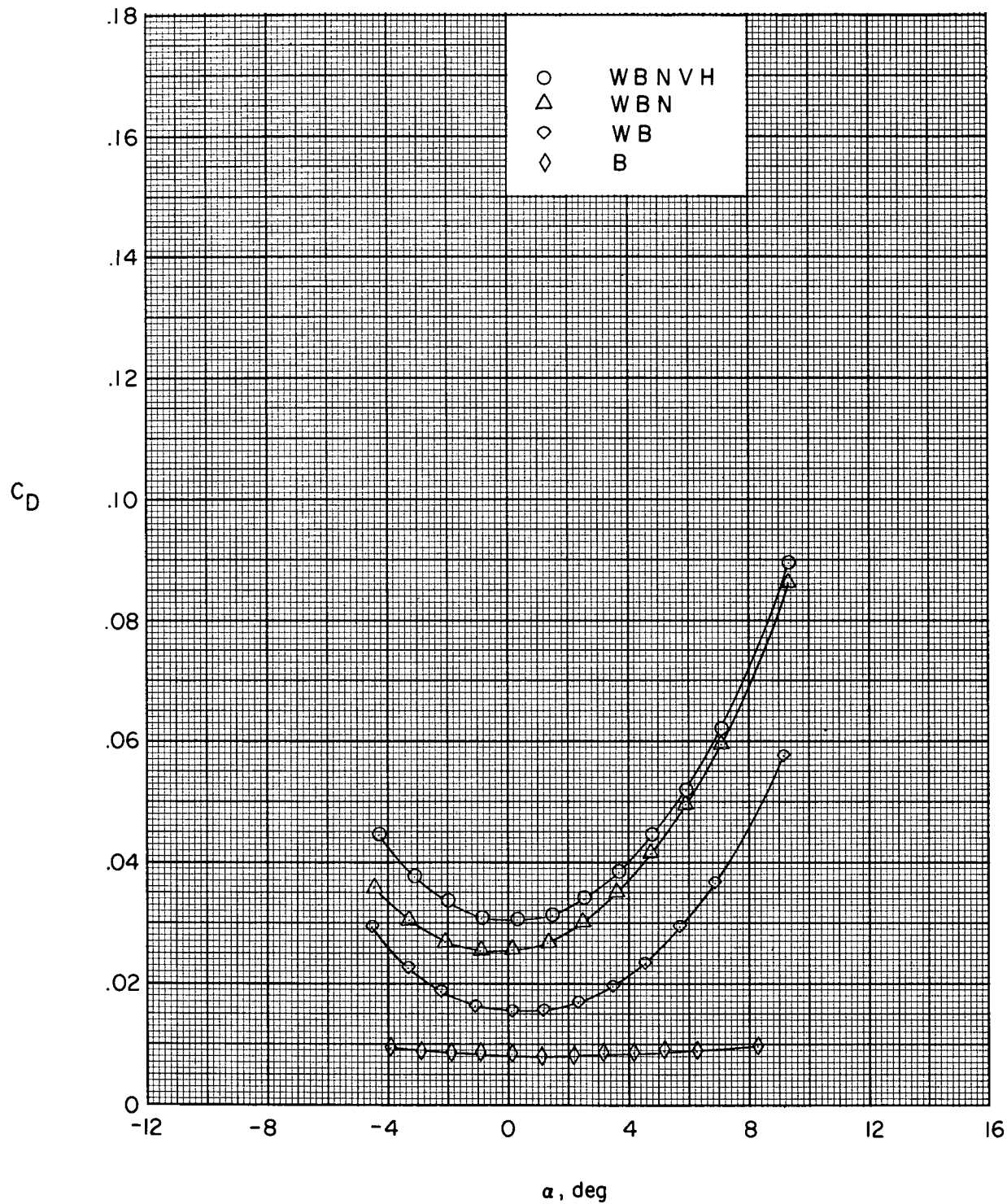


Figure 2.- Concluded.

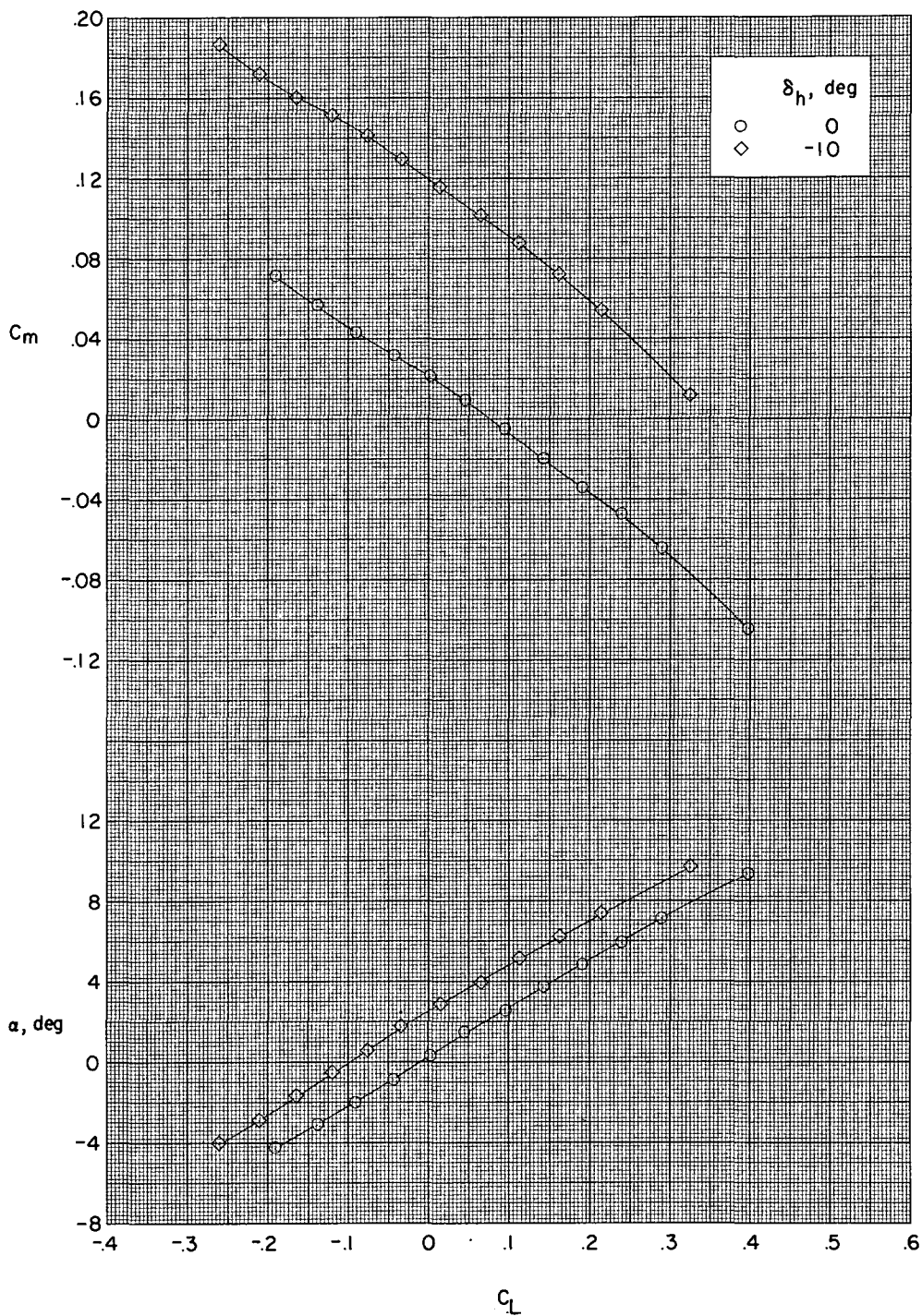


Figure 3.- Effects of horizontal-tail deflection on the longitudinal aerodynamic characteristics of the complete configuration with 80° sweptback wing panels and small horizontal outboard nacelles. $M = 1.41$.

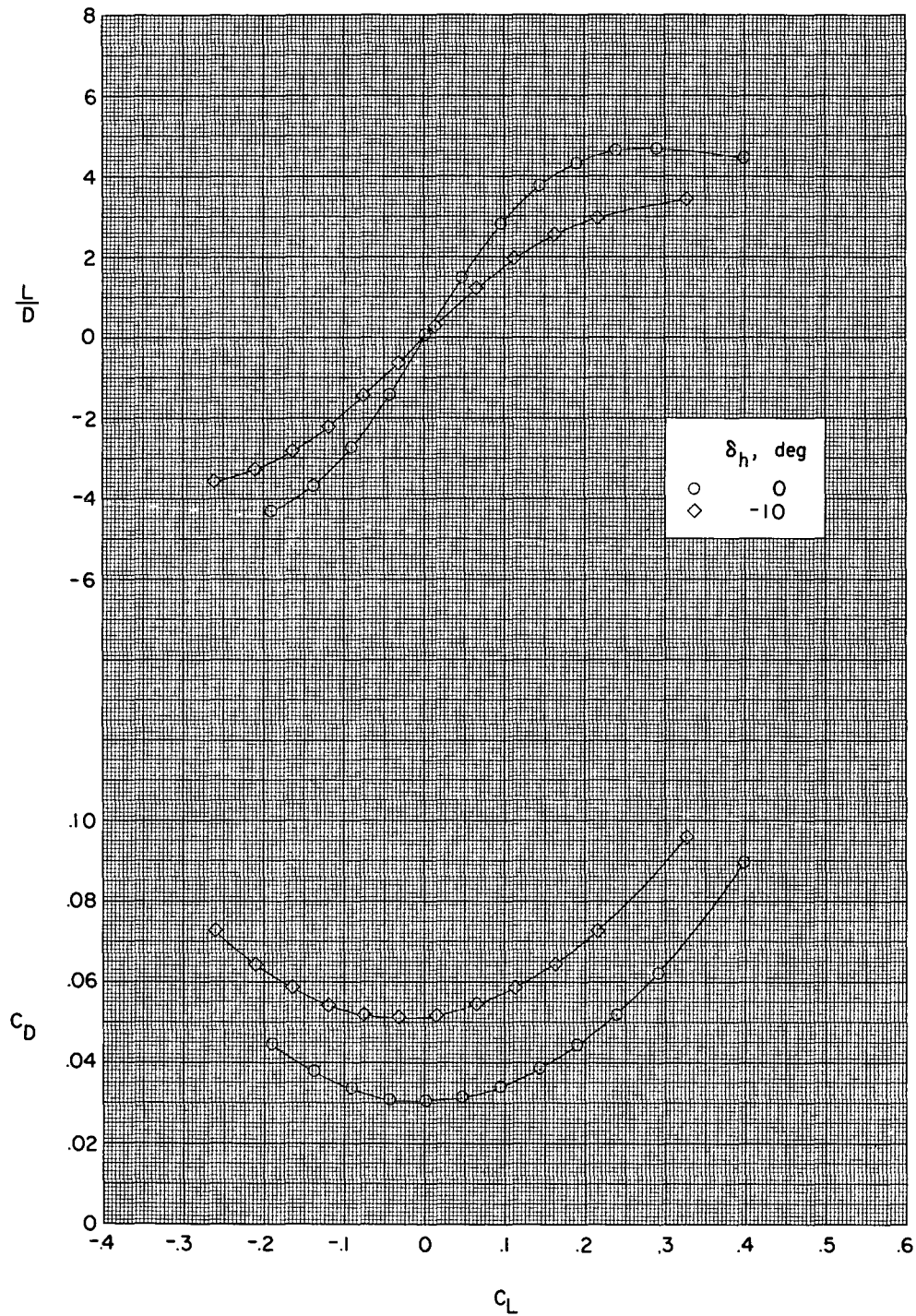


Figure 3.- Concluded.

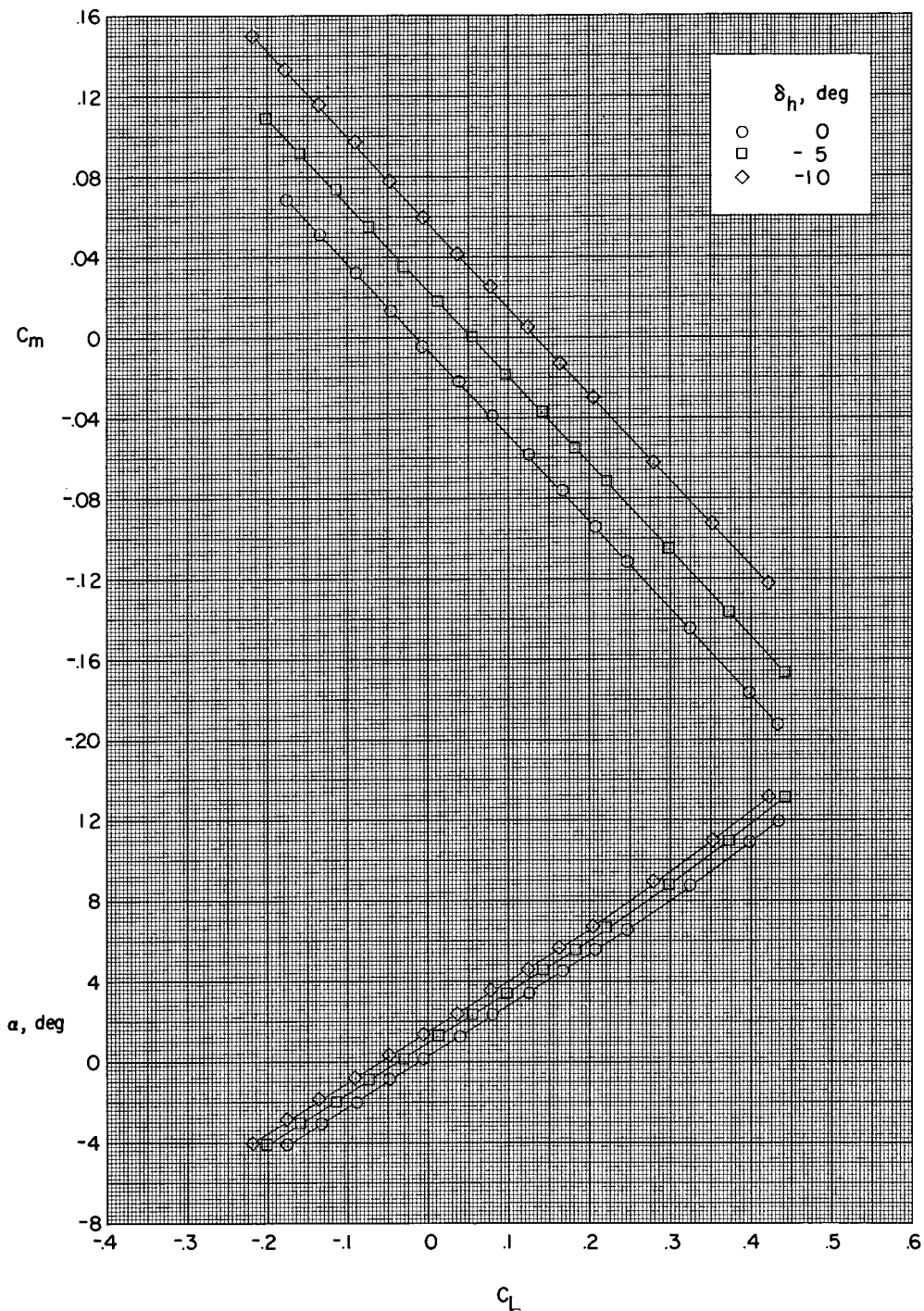


Figure 4.- Effect of horizontal-tail deflection on the longitudinal aerodynamic characteristics of the complete configuration with 65° sweptback wings and small horizontal outboard nacelles. $M = 2.20$.

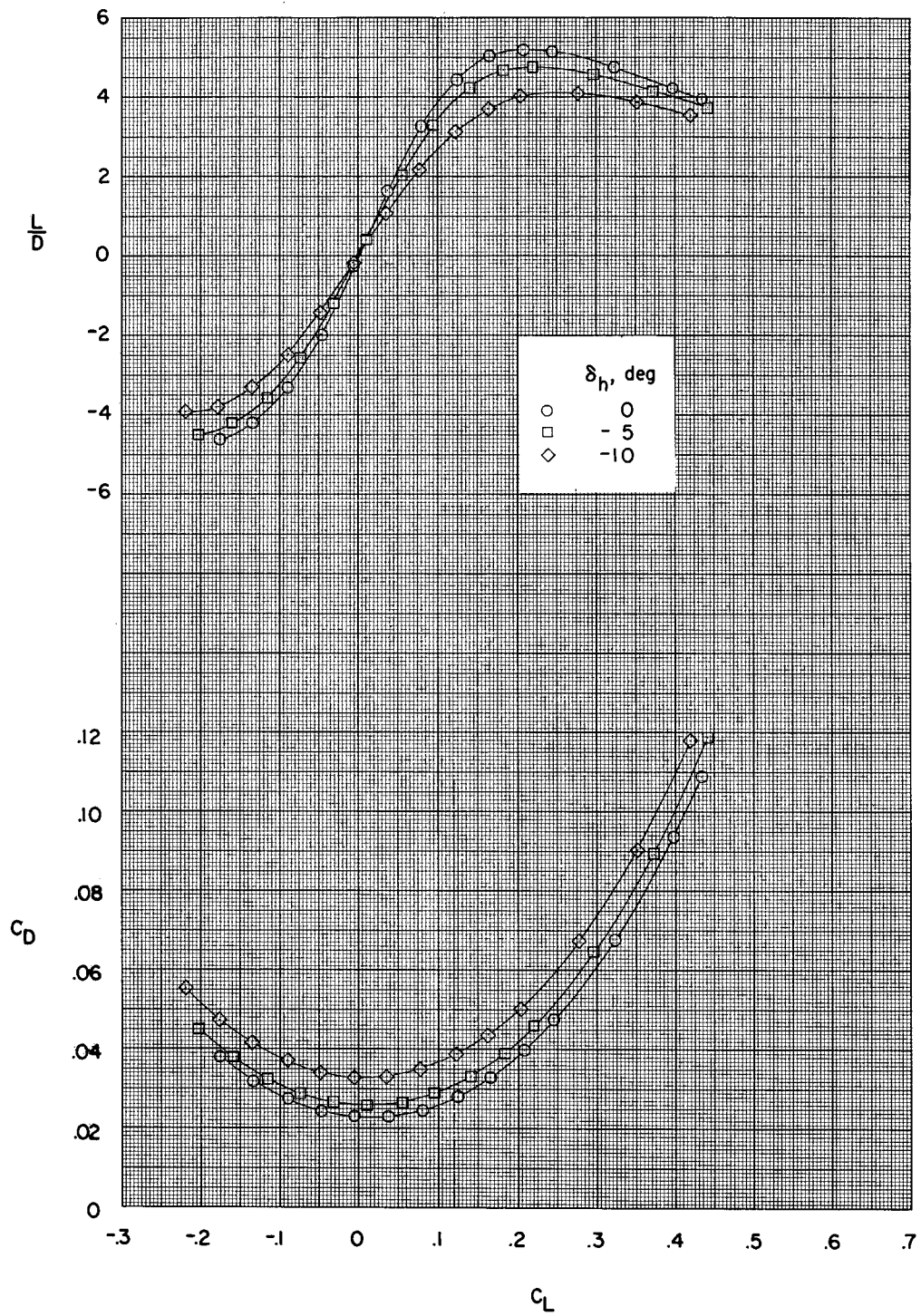


Figure 4.- Concluded.

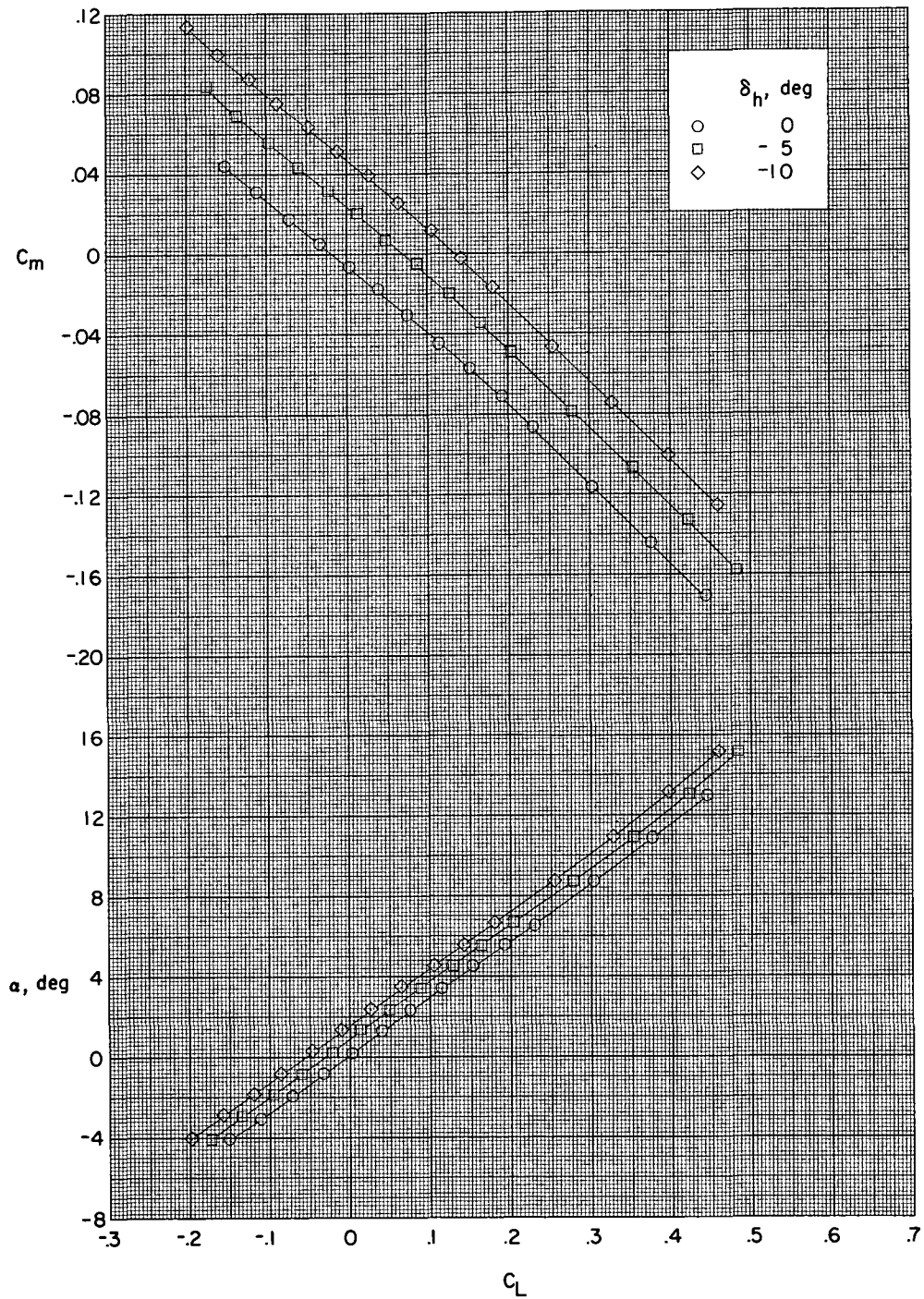


Figure 5.- Effect of horizontal-tail deflection on the longitudinal aerodynamic characteristics of the complete configuration with 80° sweptback wing and small horizontal outboard nacelles. $M = 2.20$.

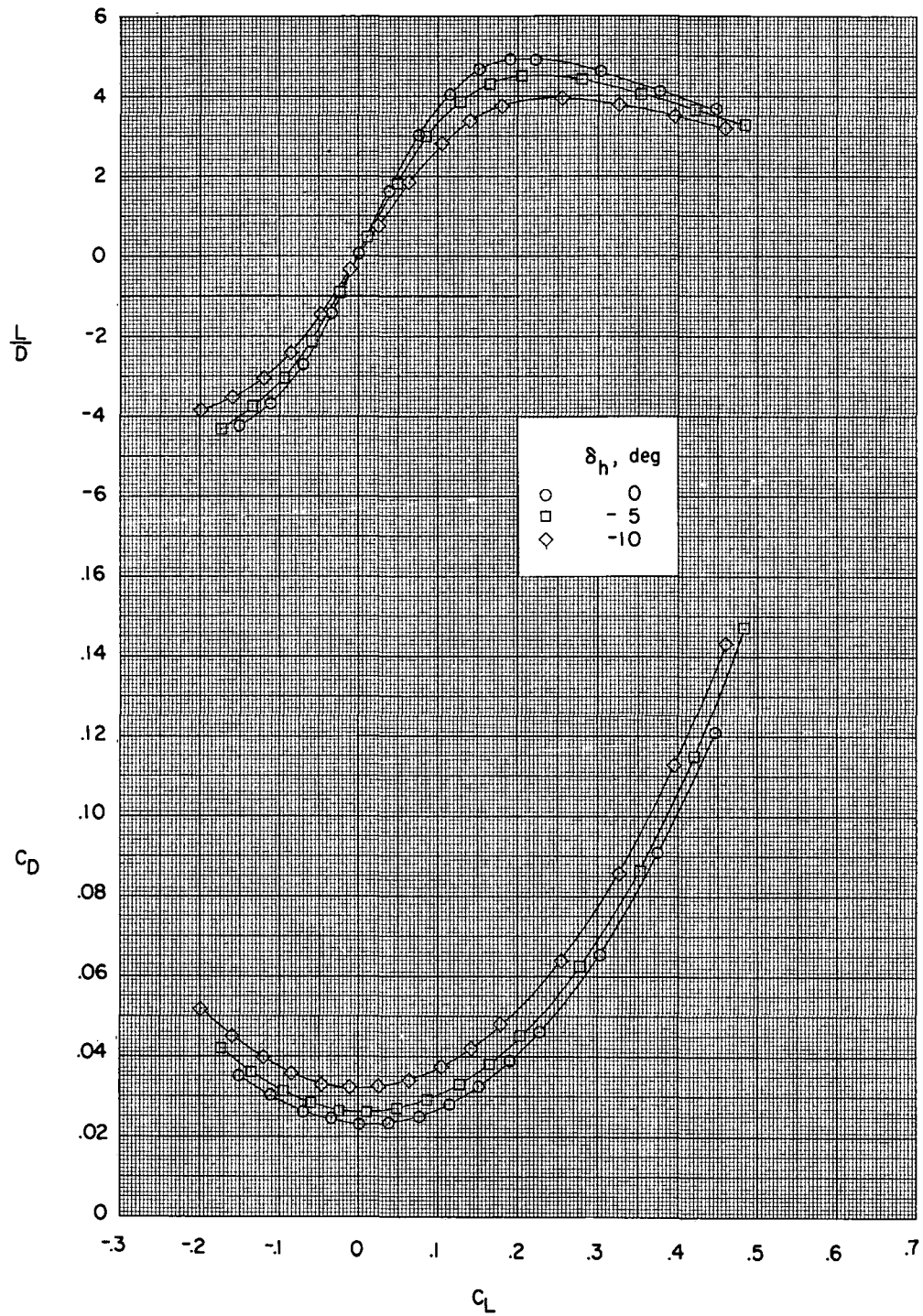


Figure 5.- Concluded.

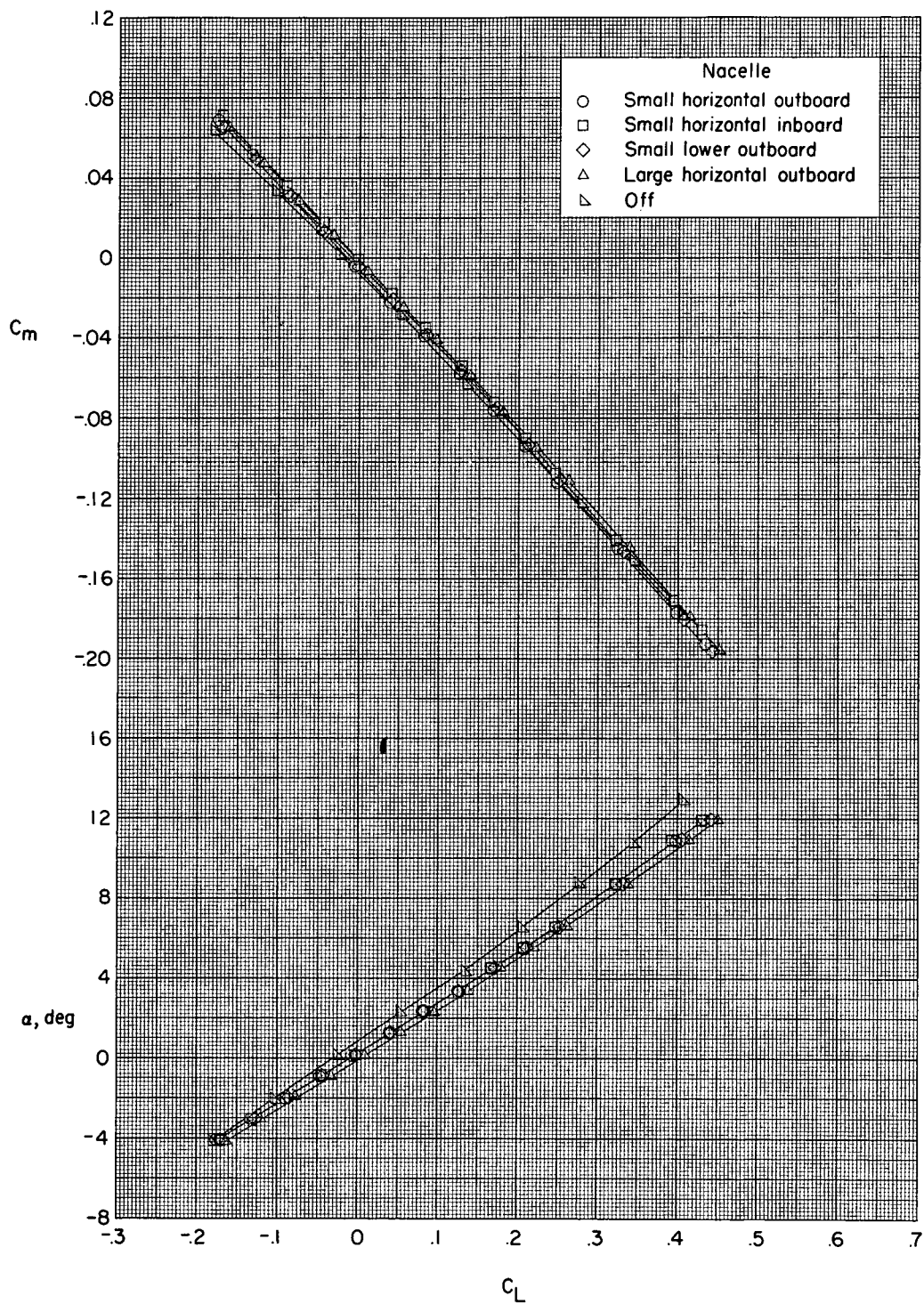


Figure 6.- Effects of various nacelles and nacelle positions on the longitudinal aerodynamic characteristics of model with 65° sweptback wing. $M = 2.20$.

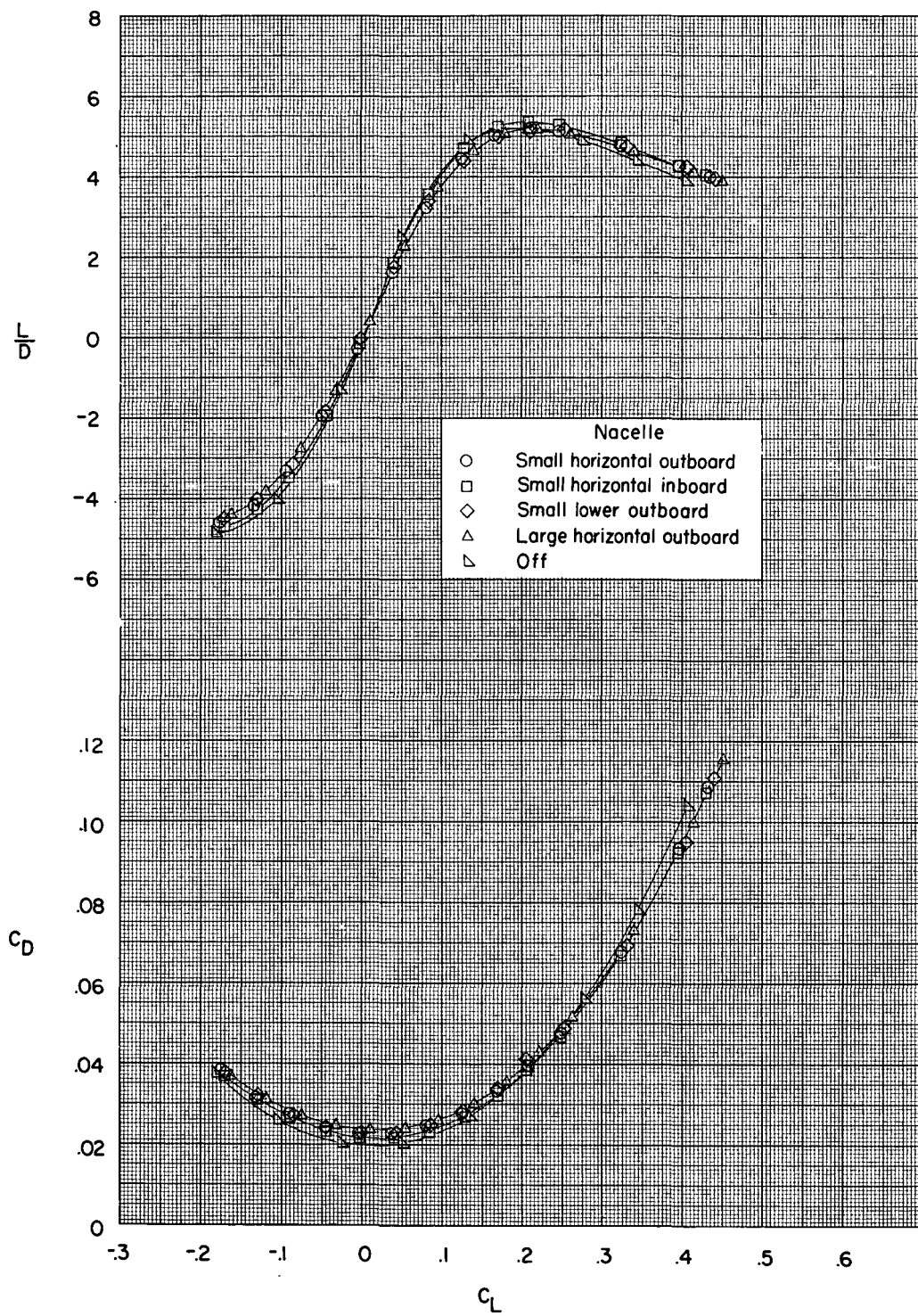
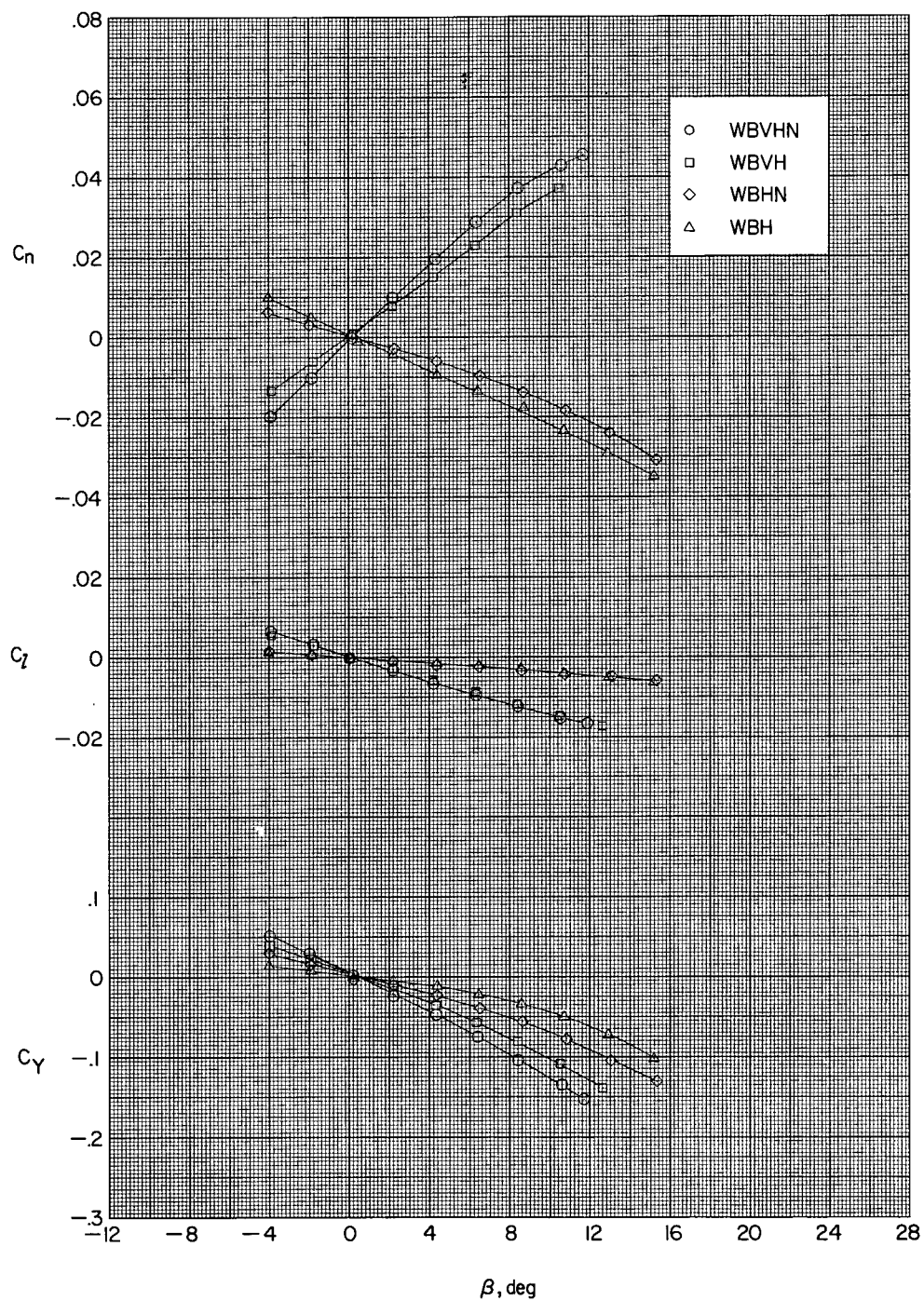
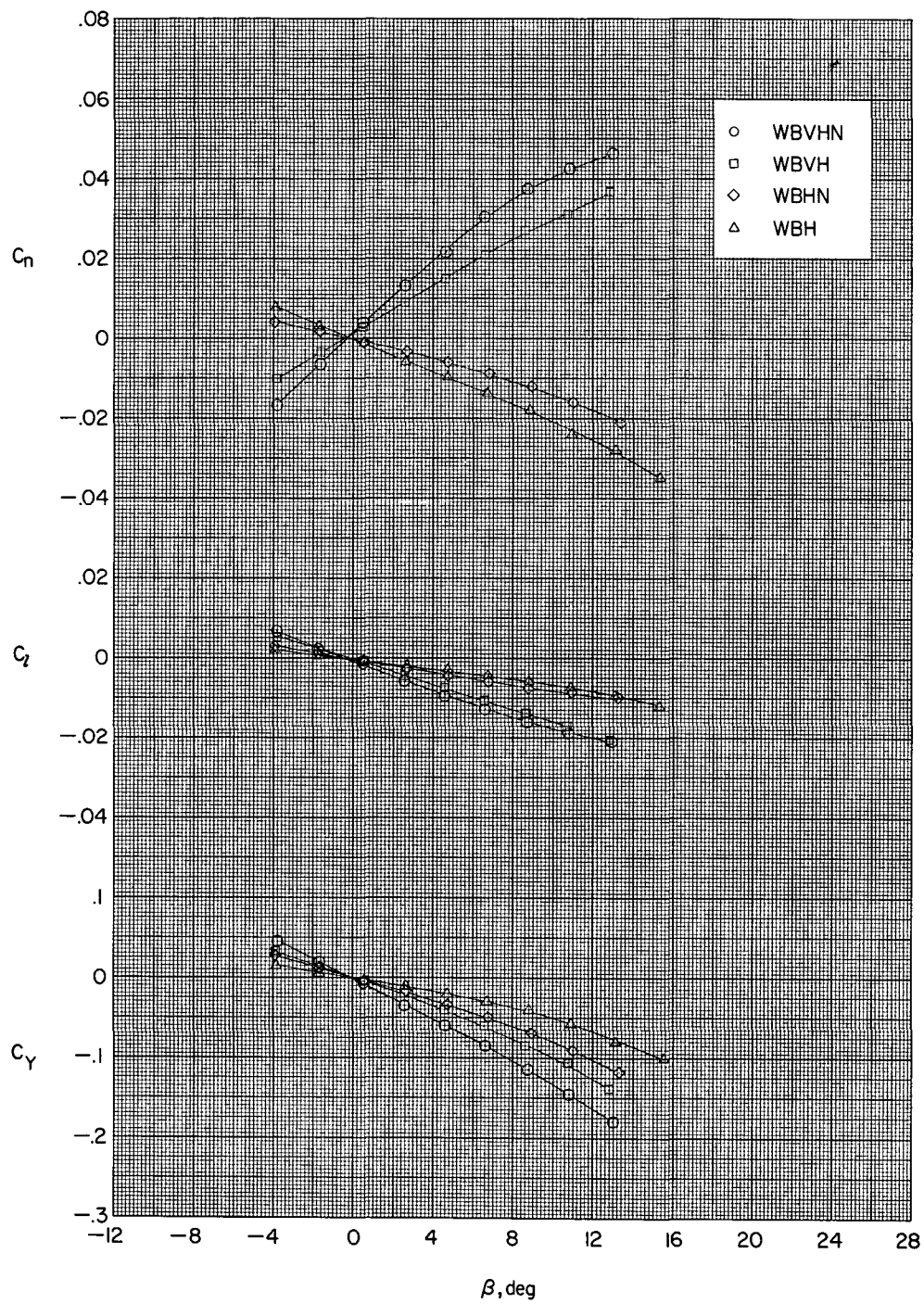


Figure 6.- Concluded.



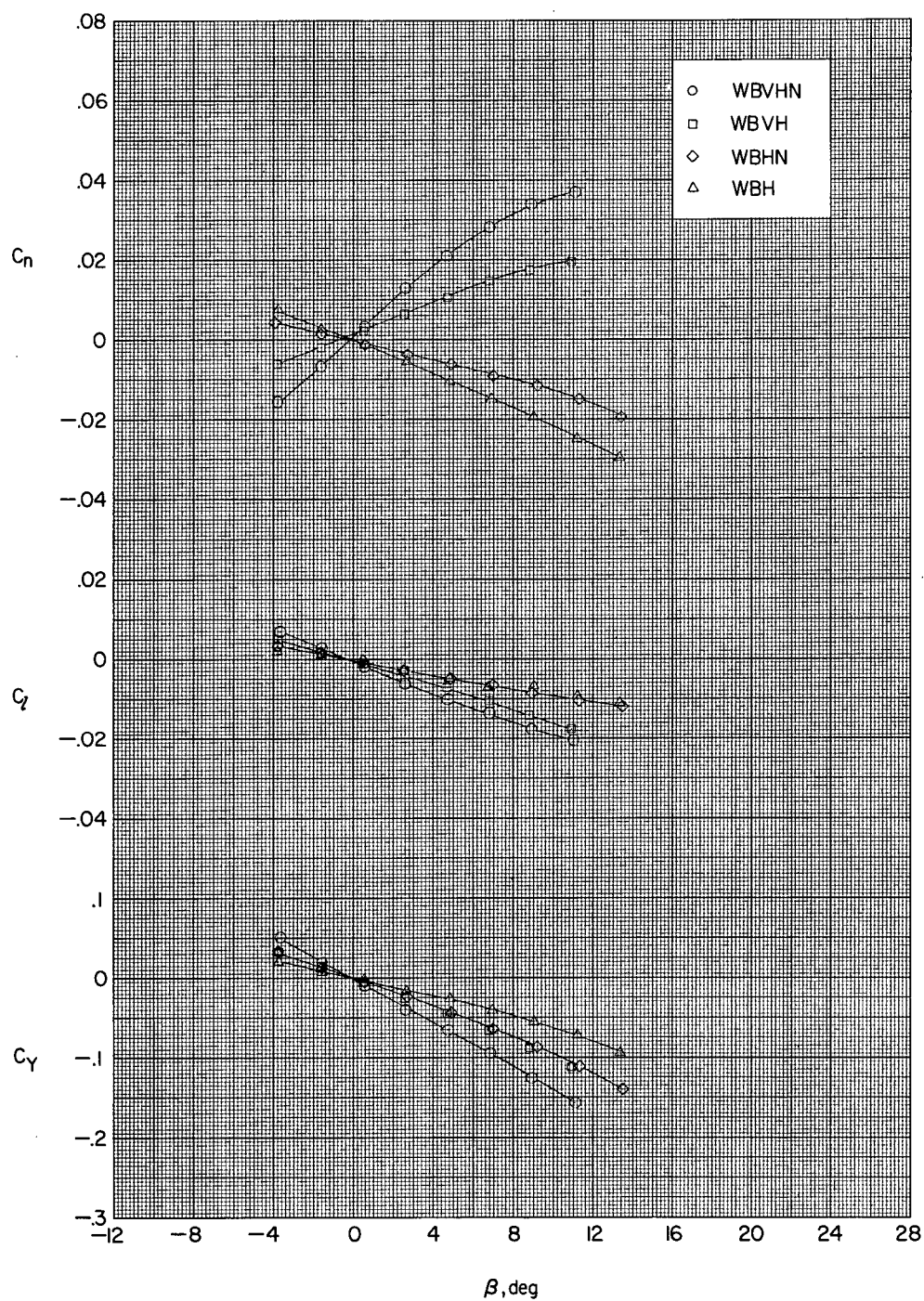
(a) $\alpha = -0.1^\circ$.

Figure 7.- Effect of vertical tail on lateral aerodynamic characteristics of model with and without small horizontal outboard nacelles. $\Lambda = 65^\circ$; $M = 2.20$.



(b) $\alpha = 4.3^\circ$.

Figure 7.- Continued.



(c) $\alpha = 8.6^\circ$.

Figure 7.- Concluded.

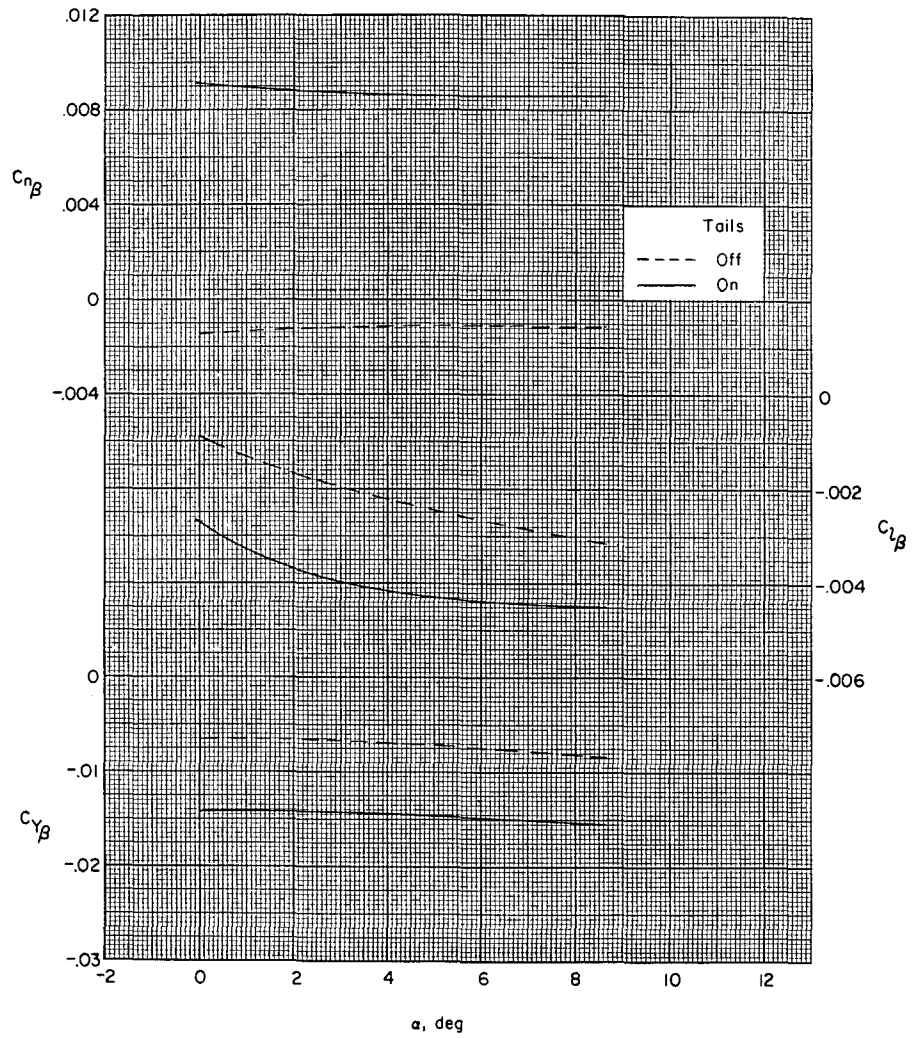


Figure 8.- Effect of vertical and horizontal tails on lateral stability derivatives of model with small horizontal outboard nacelles. $\Lambda = 80^\circ$; $M = 1.41$.

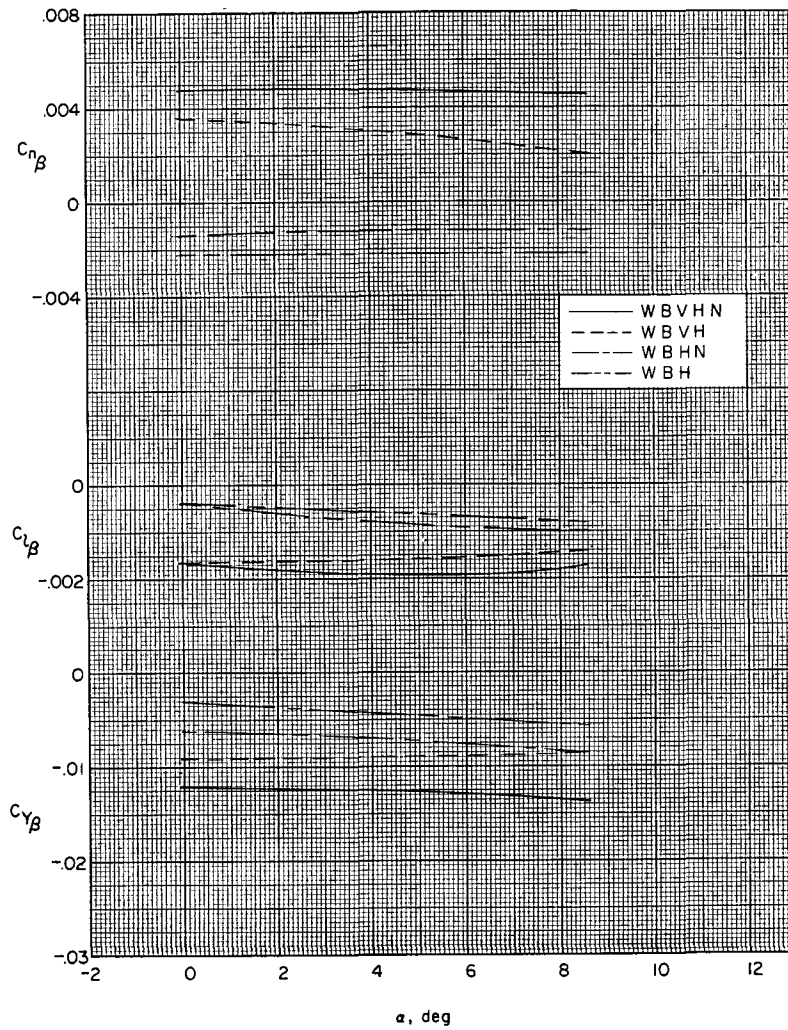


Figure 9.- Effect of vertical tail on lateral stability derivatives of model with and without small horizontal outboard nacelles. $\Lambda = 65^\circ$; $M = 2.20$.

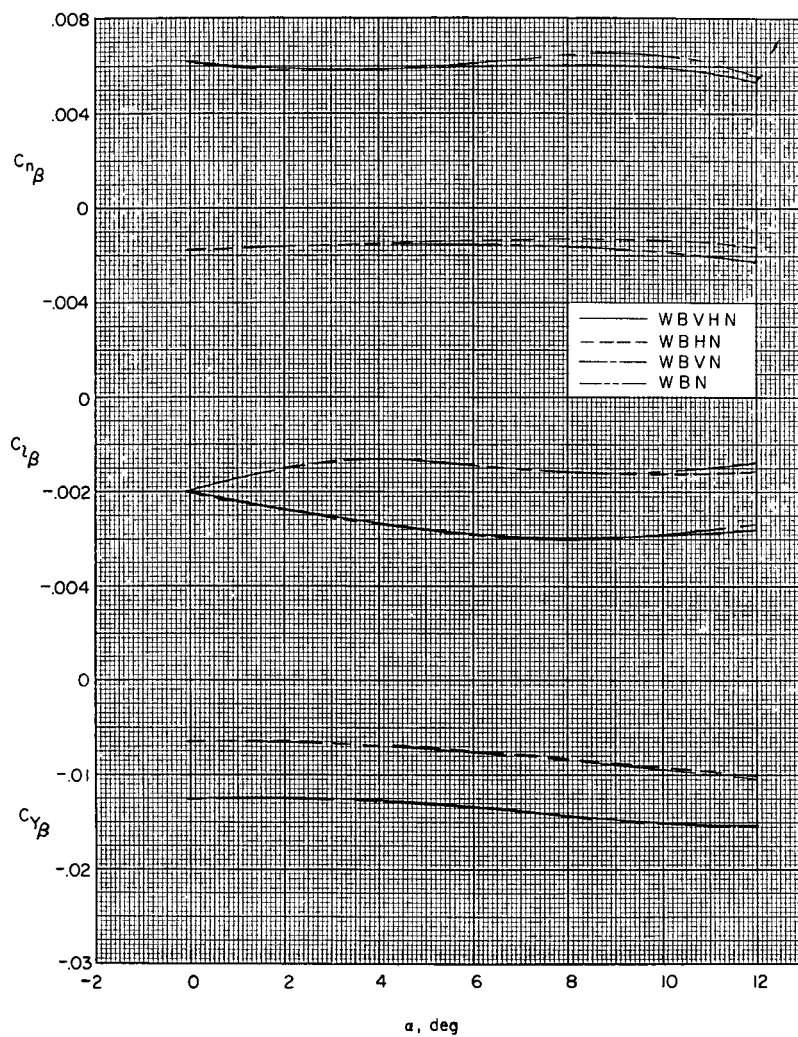


Figure 10.- Effects of vertical and horizontal tails on lateral stability derivatives of model with and without small horizontal outboard nacelles. $\Lambda = 80^\circ$; $M = 2.20$.